

Gas-Phase Coordination of Mg^+ , $(c\text{-C}_5\text{H}_5)\text{Mg}^+$, and $(c\text{-C}_5\text{H}_5)_2\text{Mg}^+$ with Saturated Hydrocarbons

Rebecca K. Milburn, Maxim V. Frash, Alan C. Hopkinson, and Diethard K. Bohme*

Department of Chemistry and Centre for Research in Earth and Space Science, York University, North York, Ontario, Canada, M3J 1P3

Received: September 27, 1999; In Final Form: February 1, 2000

The coordination of the electronic ground states of Mg^+ , $(c\text{-C}_5\text{H}_5)\text{Mg}^+$, and $(c\text{-C}_5\text{H}_5)_2\text{Mg}^+$ with the straight-chain saturated hydrocarbons methane, ethane, *n*-propane, *n*-butane, *n*-pentane, *n*-hexane, and *n*-heptane has been investigated in the gas phase in helium at room temperature and moderate pressures. Reaction rate coefficients and product distributions were measured with the selected-ion flow tube (SIFT) technique operating at 294 ± 3 K and a helium buffer-gas pressure of 0.35 ± 0.01 Torr. Rate coefficients were measured for all observed ligation steps (or upper limits in the case of nonreactions), and bond connectivities in the coordinated ions were probed with multicollision-induced dissociation. Only single ligation was observed. The rate of ligation was found to depend on the size of the saturated hydrocarbon, increasing with increasing size until the collision rate is reached, and on the degree of ligation with *c*- C_5H_5 . Mg^+ was found to be unreactive with methane and ethane, $k < 10^{-13}$ cm^3 molecule $^{-1}$ s $^{-1}$, but ligation was observed with the other hydrocarbons, $k \geq 7 \times 10^{-12}$ cm^3 molecule $^{-1}$ s $^{-1}$. Single ligation of Mg^+ with *c*- C_5H_5 substantially enhances the efficiency of subsequent ligation: the ligation is rapid, $k \geq 1.4 \times 10^{-10}$ cm^3 molecule $^{-1}$ s $^{-1}$, with all the saturated hydrocarbons investigated. Double ligation with *c*- C_5H_5 completely shuts down the efficiency of ligation: no reaction was observed between the saturated hydrocarbons and the full-sandwich magnesocene cation, $k < 10^{-13}$ cm^3 molecule $^{-1}$ s $^{-1}$. A linear correlation is reported between the measured thresholds for multicollision-induced dissociation and the polarizability of the hydrocarbon ligand. With a view to published calculations by Bauschlicher et al. for $\text{Mg}^+\text{-CH}_4$ and $\text{Mg}^+\text{-C}_2\text{H}_4$, this correlation is consistent with end-on structures for the $\text{Mg}^+\text{-L}$ and $(c\text{-C}_5\text{H}_5)\text{Mg}^+\text{-L}$ species observed in this study. A detailed study using density functional theory for the interaction of Mg^+ with three rotamers of *n*-pentane indicates that interconversion of different isomers of $\text{Mg}^+\text{-}n\text{-C}_5\text{H}_{12}$ should be easy, even at room temperature and that the ligated species $\text{Mg}^+\text{-}n\text{-C}_5\text{H}_{12}$ is “dynamic” rather than “static”. Stronger bonding (by a factor of about two) is indicated for $(c\text{-C}_5\text{H}_5)\text{Mg}^+\text{-L}$ by the multicollision CID experiments, and this is consistent with a formal description of $(c\text{-C}_5\text{H}_5)\text{Mg}^+$ as $(c\text{-C}_5\text{H}_5)^-\text{Mg}^{2+}$.

Introduction

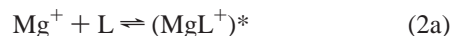
Early studies of the gas-phase chemistry of magnesium ions were focused on the reactivity of this ion toward atmospheric inorganic molecules because of the importance of this chemistry in the earth's ionosphere.^{1–3} More recently, interests have shifted toward organomagnesium ion chemistry, particularly as it is thought to proceed in meteor trains,⁴ the atmospheres of stars,⁵ and the atmospheres of Neptune and the other giant planets.⁶ Of course, there is also an ongoing interest in fundamental physicochemical aspects of organomagnesium chemistry. Thus, binding energies have been measured for the ligation of Mg^+ with a series of alcohols, aldehydes, ethers, and ketones using Fourier transform mass spectrometry (FTMS).⁷ Experimental measurements of the kinetics of reactions of Mg^+ with a variety of organic molecules using a selected-ion flow tube (SIFT)/glow discharge technique have been initiated in the laboratory of Babcock.⁸ Also, theoretical studies of the energetics for the ligation of Mg^+ with methane and ethane have been reported recently by Bauschlicher and co-workers.^{9,10}

Our own investigations of gas-phase organomagnesium ion chemistry have focused first on SIFT measurements of the reactions of the organometallic ions $(c\text{-C}_5\text{H}_5)\text{Mg}^+$ and $(c\text{-C}_5\text{H}_5)_2\text{Mg}^+$ with inorganic molecules and how these compare to

reactions of bare Mg^+ ions.^{11,12} Here, we report systematic SIFT investigations of the reactivity of Mg^+ toward saturated hydrocarbon molecules and of changes in Mg^+ reactivity upon ligation with one and two cyclopentadienyl radicals. The Mg^+ , $(c\text{-C}_5\text{H}_5)\text{Mg}^+$, and $(c\text{-C}_5\text{H}_5)_2\text{Mg}^+$ ions were generated from magnesocene by electron-impact ionization and were allowed to thermalize by collisional deactivation with He atoms prior to reaction. The reactivities of these ions were assessed through measurements of rate coefficients for ligation at room temperature and at operating helium pressures that are sufficiently high to allow collisional stabilization of the ligated ions. Under such operating conditions, ligation occurs by termolecular reactions such as those in eq 1



Rate coefficients for such ligation reactions are sensitive to the ligand bond energy $D(\text{Mg}^+\text{-L})$ and the size of the ligand. This is because the gas-phase ligation proceeds in two steps, eq 2a,b, and the lifetime of the intermediate $(\text{MgL}^+)^*$ against dissociation



back to reactants is dependent both on the degrees of freedom in $(\text{MgL}^+)^*$ effective in intramolecular energy redistribution in the transient intermediate and on its attractive well depth, $D(\text{Mg}^+-\text{L})$.¹³ The family of saturated hydrocarbons chosen for this study provides a wide range both in degrees of freedom and in ligand binding energy.

When the energy of ligation becomes sufficiently small, the reverse reaction (reverse of eq 1) may become significantly fast and drive the ligation reaction of eq 1 toward equilibrium. In such instances, an equilibrium data analysis can provide a measure of the standard free energy of ligation. This has been achieved here for several reactions leading to weak ligation. Also, the ligated MgL^+ ions observed were explored with multicollision-induced dissociation (CID) experiments.¹⁴ Such experiments provide indications of bond connectivities in the stabilized ligated species MgL^+ as well as estimates of relative Mg^+-L bond strengths.

Experimental Section

The results reported here were obtained using a selected-ion flow tube (SIFT) apparatus that has been described previously.^{15,16} All measurements were performed at 294 ± 3 K and at a helium buffer gas pressure of 0.35 ± 0.01 Torr. The reactant ions, Mg^+ , $(c\text{-C}_5\text{H}_5)\text{Mg}^+$, and $(c\text{-C}_5\text{H}_5)_2\text{Mg}^+$ were all generated in a low-pressure ion source from the vapor of magnesocene (Sigma-Aldrich, 97%) by electron impact ionization at electron energies of 35, 50, and 10 eV, respectively. Some collisional dissociation of $(c\text{-C}_5\text{H}_5)_2\text{Mg}^+$ and $(c\text{-C}_5\text{H}_5)\text{Mg}^+$ was observed to accompany ion injection into the flow tube: about 75% of the full sandwich fragmented to the half sandwich, while about 18% of the half sandwich broke to form Mg^+ in the flow tube. The injected ions were thermalized by collisions (about 4×10^5) with helium buffer gas before entering the reaction region further down stream. Reactant neutrals were introduced into the reaction region as a dilute 10% mixture in helium and had the following purity: methane (Matheson, 99.97%), ethane (Matheson, 99.99%), *n*-propane (Air Products, 99.5%), *n*-butane (Matheson, 99%), *n*-pentane, *n*-hexane, and *n*-heptane (all three Sigma-Aldrich HPLC grade, +99%). The rate coefficients and product distributions were measured in the usual manner.^{15,16} The rate coefficients are estimated to have an absolute accuracy of $\pm 30\%$. When appropriate, a check was made for approach to equilibrium by plotting the ratio of the product ion to the reactant ion concentrations versus reactant neutral concentration. When equilibrium is achieved, such a plot becomes linear and the rate coefficient in the forward direction determined by fitting is regarded as a lower limit to the true value. Bond connectivities in the product ions were investigated with CID experiments by raising the sampling nose-cone voltage from 0 to -80 V while concomitantly varying the potentials of front and rear quadrupole focusing lenses so as not to introduce mass discrimination.¹⁴

Computational Methods

The computations were carried out with the Gaussian 98 program.¹⁷ The hybrid density functional method, B3LYP,^{18–20} was used in conjunction with a large basis set, 6-311++G(2d,2p). The computed enthalpies of interaction include electronic terms, BSSE corrections (taken from the counterpoise calculations), zero-point contributions, and thermal contributions (the latter two obtained from the frequency calculations). The frequency calculations also provided the entropy changes.

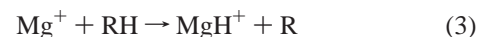
To check precision of the selected method, test calculations on the interaction of ethane (end-on and side-on complexes)¹⁰ with Mg^+ were performed. Their results indicated that further enlargement of the basis set does not significantly affect the

results. Single-point interaction energies computed at B3LYP/6-311++G(3df,3pd) are only $0.5\text{--}0.6$ kcal mol⁻¹ higher than those at B3LYP/6-311++G(2d,2p). Use of the high-level *ab initio* coupled cluster functional^{21,22} instead of B3LYP also did not significantly change the results. The CCSD(T)(full)/6-311++G(2d,2p)//B3LYP/6-311++G(2d,2p) interaction energies are only $0.5\text{--}0.6$ kcal mol⁻¹ lower than those at B3LYP/6-311++G(2d,2p).

Results and Discussion

Table 1 summarizes, in order of increasing molecular weight of the reactant, the rate coefficients measured for reactions of Mg^+ , $(c\text{-C}_5\text{H}_5)\text{Mg}^+$, and $(c\text{-C}_5\text{H}_5)_2\text{Mg}^+$ with the saturated hydrocarbons selected for study. All rate coefficients are *apparent* bimolecular rate coefficients at 294 ± 3 K and a helium buffer-gas pressure of 0.35 ± 0.01 Torr. Ionization energies and standard enthalpy changes referred to in the text were derived from the values found in the NIST Chemistry Web Book²⁴ unless indicated otherwise.

A. Mg^+ Reactions. Mg^+ was found to be unreactive with methane and ethane, $k < 10^{-13}$ cm³ molecules⁻¹ s⁻¹, but it did react measurably with *n*-propane, *n*-butane, *n*-pentane, *n*-hexane, and *n*-heptane. Measurements taken for the reaction of Mg^+ with *n*-propane, *n*-butane, *n*-pentane, and *n*-hexane are shown in Figure 1. Only *single* ligation according to eq 1 was observed. No bimolecular products, as might arise, for example, from hydrogen atom transfer or hydride transfer reactions such as those shown in eqs 3 and 4, were detected



The thermochemistry of these two particular bimolecular channels can be evaluated for the lower hydrocarbons when adopting the computed standard enthalpies of formation for MgH^+ (220 kcal mol⁻¹) and MgH (57 kcal mol⁻¹) reported by Gardner et al.²⁵ With RH = methane or ethane, for example, eqs 3 and 4 are endothermic by at least 55 and 75 kcal mol⁻¹,

TABLE 1: Measured Rate Coefficients for Reactions of the Ground States of Mg^+ , $(c\text{-C}_5\text{H}_5)\text{Mg}^+$ and $(c\text{-C}_5\text{H}_5)_2\text{Mg}^+$ with Straight-Chain Saturated Hydrocarbons Preceding at 294 ± 3 K in Helium Buffer Gas at a Total Pressure of 0.35 ± 0.01 Torr^a

ligand	Mg^+	$(c\text{-C}_5\text{H}_5)\text{Mg}^+$	$(c\text{-C}_5\text{H}_5)_2\text{Mg}^+$
methane	NR ^b , $<10^{-13}$	1.4×10^{-10}	NR, $<10^{-13}$
CH ₄	$[1.22 \times 10^{-9}]$	$[1.02 \times 10^{-9}]$	$[0.98 \times 10^{-9}]$
ethane	NR, $<10^{-13}$	9.5×10^{-10}	NR, $<10^{-13}$
C ₂ H ₆	$[1.35 \times 10^{-9}]$	$[1.05 \times 10^{-9}]$	$[0.99 \times 10^{-9}]$
<i>n</i> -propane	$\geq 7.1 \times 10^{-12}$	1.0×10^{-9}	NR, $<10^{-13}$
<i>n</i> -C ₃ H ₈	$[1.49 \times 10^{-9}]$	$[1.08 \times 10^{-9}]$	$[1.00 \times 10^{-9}]$
<i>n</i> -butane	1.4×10^{-10}	1.0×10^{-9}	NR, $<10^{-13}$
<i>n</i> -C ₄ H ₁₀	$[1.63 \times 10^{-9}]$	$[1.13 \times 10^{-9}]$	$[1.03 \times 10^{-9}]$
<i>n</i> -pentane	4.9×10^{-10}	1.1×10^{-9}	NR, $<10^{-13}$
<i>n</i> -C ₅ H ₁₂	$[1.75 \times 10^{-9}]$	$[1.17 \times 10^{-9}]$	$[1.06 \times 10^{-9}]$
<i>n</i> -hexane	1.1×10^{-9}	1.6×10^{-9}	NR, $<10^{-13}$
<i>n</i> -C ₆ H ₁₄	$[1.87 \times 10^{-9}]$	$[1.22 \times 10^{-9}]$	$[1.09 \times 10^{-9}]$
<i>n</i> -heptane	2.0×10^{-9}	1.3×10^{-9}	NR, $<10^{-13}$
<i>n</i> -C ₇ H ₁₆	$[1.97 \times 10^{-9}]$	$[1.26 \times 10^{-9}]$	$[1.11 \times 10^{-9}]$

^a Reaction and collision rate coefficients are given in units of cubic centimeters per molecule per second. All of the observed reactions are addition reactions, and the measured rate coefficients are effective bimolecular rate coefficients. The relative uncertainty in all reaction rate coefficient does not exceed 10%; however, the absolute error may be as high as 30%. Collision rate coefficients are given in square brackets and calculated using TC theory.²³ ^b NR denotes no reaction.

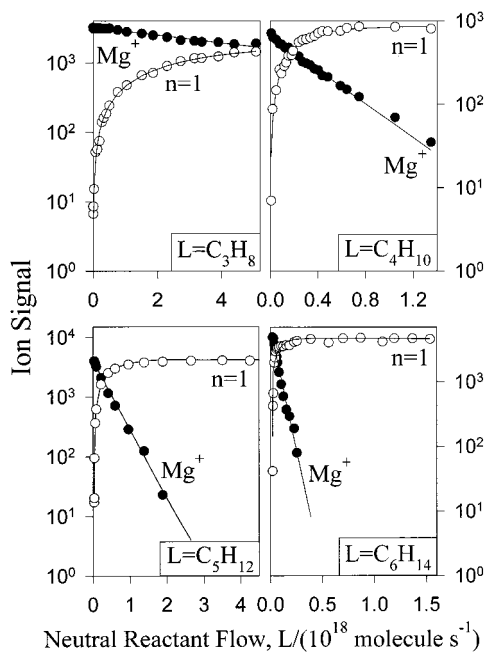
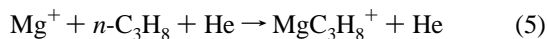


Figure 1. Composite of kinetic data obtained for reactions of Mg^+ to produce MgL_n^+ with $L = n$ -propane, n -butane, n -pentane, and n -hexane. The measurements were performed at 294 ± 3 K and at a helium buffer-gas pressure of 0.35 ± 0.01 Torr. The solid lines represent a computer fit of the experimental data with the solution of the appropriate differential equations.

respectively. Also, the transfer of an electron to Mg^+ is endothermic for all the saturated hydrocarbons investigated even though $\text{IE}(\text{RH})$ decreases as the size of the hydrocarbon increases. $\text{IE}(\text{RH})$ decreases from 12.61 eV for methane to $\text{IE} = 9.93$ eV for n -heptane and so approaches, but never falls below, that of Mg , $\text{IE}(\text{Mg}) = 7.65$ eV.

Our observations are only partially in agreement with the preliminary qualitative results of Linder et al.⁸ who reported ligation with n -propane and n -butane as well as ethane under similar SIFT conditions in which, however, Mg^+ was produced in a glow-discharge source. No rate coefficients were reported by these authors for these reactions so that a precise comparison cannot be made. It is interesting to note that for n -propane, Linder et al.⁸ report the dependence of the effective bimolecular rate coefficient on He pressure expected for termolecular ligation reactions.

An equilibrium analysis of the kinetic data for the ligation with n -propane shows that this reaction achieves equilibrium under our SIFT conditions. This is shown in Figure 2. As a consequence the rate coefficient deduced for reaction 5 from the observed decay of Mg^+ , $k = 7.1 \times 10^{-12} \text{ cm}^3 \text{ molecules}^{-1} \text{ s}^{-1}$,



must be regarded as a lower limit. The ion-signal ratio plot in Figure 2 yields an equilibrium constant for eq 5, $K_{\text{eq}} = 1.2 \times 10^6$, that corresponds to a standard free-energy change, $\Delta G^\circ = -8.3 \text{ kcal mol}^{-1}$. In comparison, the ligation reactions with n -butane and higher homologues do not achieve equilibrium, $K_{\text{eq}} \geq 1.2 \times 10^8$, and therefore have standard free-energy changes, $-\Delta G^\circ \geq 11.0 \text{ kcal mol}^{-1}$.

Figure 3 displays the multicollision CID spectra obtained for MgL^+ with $L = n$ -propane, n -butane, n -pentane, and n -hexane. All onsets for dissociation occur at relatively low voltages. The

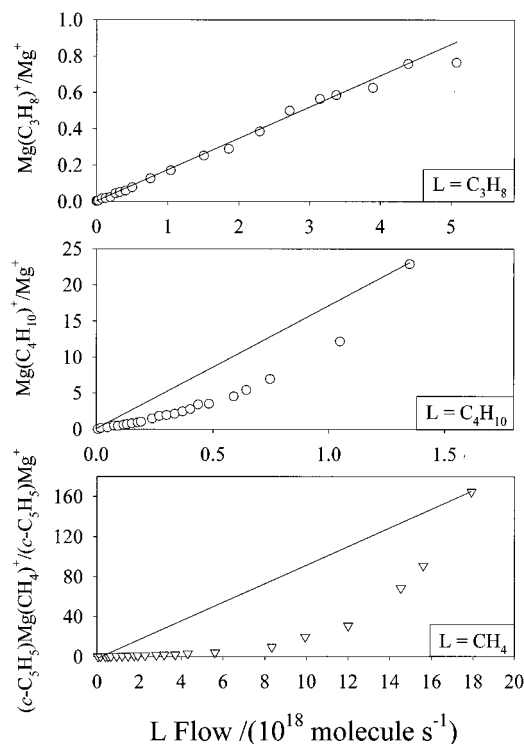


Figure 2. Ion-signal ratio plots showing the approach to, and attainment of, equilibrium for the ligation reactions of Mg^+ with n -propane and n -butane and of $(c\text{-C}_3\text{H}_5)\text{Mg}^+$ with methane.

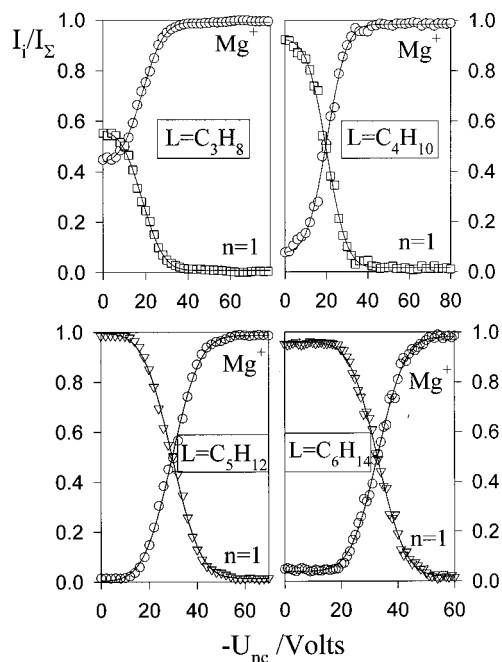


Figure 3. Composite of multicollision CID data for the MgL_n^+ species produced in the experiments shown in Figure 1 at flows for n -propane of $6.0 \times 10^{18} \text{ molecules s}^{-1}$, for n -butane of $6.2 \times 10^{17} \text{ molecules s}^{-1}$, for n -pentane of $3.0 \times 10^{18} \text{ molecules s}^{-1}$ and for n -hexane of $3.0 \times 10^{17} \text{ molecules s}^{-1}$. U_{nc} is the nose-cone voltage.

early onset of dissociation observed with these hydrocarbons indicates weak bonding. The onsets are not well-defined for the weakest of these bonds, those with n -propane, n -butane, and n -pentane, but together with the higher onsets measured for n -hexane and n -heptane, they suggest a trend of increasing ligand-binding energy with increasing size of the hydrocarbon.

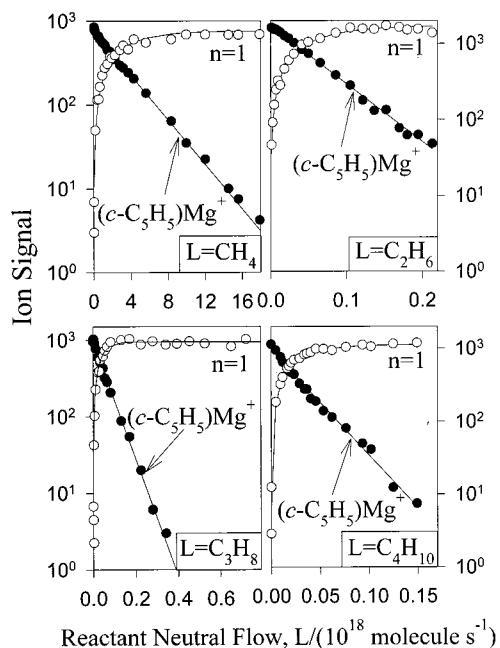
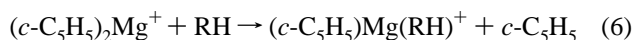


Figure 4. Composite of kinetic data obtained for reactions of $(c\text{-C}_5\text{H}_5)\text{Mg}^+$ to produce $(c\text{-C}_3\text{H}_5)\text{MgL}_n^+$ with $L =$ methane, ethane, n -propane, and n -butane. The measurements were performed at 294 ± 3 K and at a helium buffer-gas pressure of 0.35 ± 0.01 Torr. The solid lines represent a computer fit of the experimental data with the solution of the appropriate differential equations.

B. $(c\text{-C}_5\text{H}_5)\text{Mg}^+$ Reactions. Figure 4 demonstrates that $(c\text{-C}_5\text{H}_5)\text{Mg}^+$ is generally reactive with the saturated hydrocarbons investigated and ligates more efficiently than Mg^+ . Again, only single ligation was observed, and there was no evidence of the formation of binary products. There is insufficient thermochemical information and the ionization energy of $(c\text{-C}_5\text{H}_5)\text{Mg}$ is not known as far as we are aware, but presumably, hydrogen atom transfer, hydride transfer, and electron transfer are again endothermic for all the saturated hydrocarbons investigated.

There is no indication from the kinetic plots of an approach to equilibrium, even with methane for which the data indicate $K_{\text{eq}} \geq 7.2 \times 10^7$, and this suggests a larger ligand binding energy with $(c\text{-C}_5\text{H}_5)\text{Mg}^+$ than that with bare Mg^+ . This result is consistent with the measured onsets for the removal of ligands with multicollision-induced dissociation. Measured CID spectra for $(c\text{-C}_5\text{H}_5)\text{Mg(L)}^+$ are shown in Figure 5 with $L =$ methane, ethane, n -propane, and n -butane. A trend of increasing onset energy with increasing size of the ligand is easily discernible from these data, much more so than was the case with Mg^+ .

C. $(c\text{-C}_5\text{H}_5)_2\text{Mg}^+$ Reactions. The full-sandwich cation $(c\text{-C}_5\text{H}_5)_2\text{Mg}^+$ was observed not to react with any of the saturated hydrocarbons, $k < 10^{-13} \text{ cm}^3 \text{ molecules}^{-1} \text{ s}^{-1}$. Ligation was not observed, nor was there any evidence for the occurrence of ligand-switching reactions of the type in eq 6 that we have previously reported for reactions of



$(c\text{-C}_5\text{H}_5)_2\text{Mg}^+$ with the inorganic ligands ammonia and water.¹¹ The failure to observe switching indicates that all of the saturated hydrocarbons ligate less strongly to $(c\text{-C}_5\text{H}_5)\text{Mg}^+$ than does $c\text{-C}_5\text{H}_5$ itself, viz., that $D_{298}((c\text{-C}_5\text{H}_5)\text{Mg}^+ - \text{RH}) < D_{298}((c\text{-C}_5\text{H}_5)\text{Mg}^+ - c\text{-C}_5\text{H}_5)$.

D. Variation in the Rate of Ligation with the Size of the Hydrocarbon Ligand. Figure 6 shows the increase in the rate

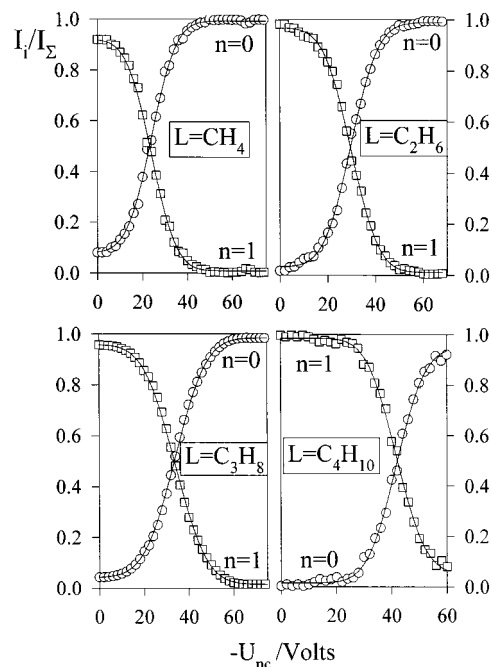


Figure 5. Composite of multicollision CID data for the $(c\text{-C}_5\text{H}_5)\text{MgL}_n^+$ species produced in the experiments shown in Figure 4 at flows for methane of 8.0×10^{18} molecules s^{-1} , ethane of 3.0×10^{17} molecules s^{-1} , n -propane of 3.0×10^{17} molecules s^{-1} , and for n -butane of 2.0×10^{17} molecules s^{-1} . U_{nc} is the nose-cone voltage.

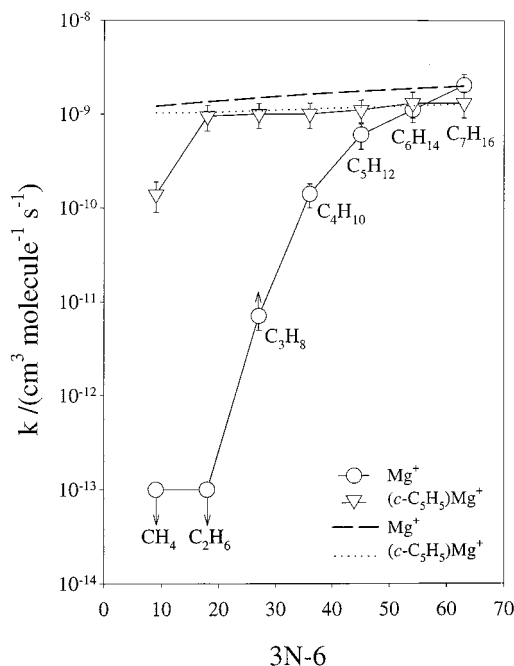


Figure 6. Variation of the effective bimolecular rate coefficient of ligation with the degrees of freedom $3N - 6$ of the ligand (N is the number of atoms). The measurements were performed at 294 ± 3 K and at a helium buffer-gas pressure of 0.35 ± 0.01 Torr. The dashed and dotted lines represent the variation of the calculated collision rate coefficient.

coefficient for ligation as a function of the size, or $3N - 6$ degrees of freedom (where N is the number of atoms), of the saturated hydrocarbon. The rate coefficient for the ligation of Mg^+ under our SIFT conditions is immeasurably small with methane and ethane, but becomes measurable for the reaction with n -propane. With n -heptane, the collision limit is achieved and no further increase in rate is expected with increasing size

of the hydrocarbon, other than that associated with the slight increase in the collision rate due to an increase in polarizability (see Table 1). The observed rise in the rate coefficient for ligation with increasing size of the hydrocarbon can be attributed to an increase in the lifetime of the transient intermediate (MgRH^+)* due to a combination of increasing binding energy and increasing degrees of freedom of the ligated ion.¹³

We attribute the enhanced rates of ligation of the half-sandwich to increased collisional stabilization of the intermediate ligated complex. The increase in collisional stabilization is a consequence of an increase in the lifetime of the intermediate complex that is expected from the increase in the ligation energy and the number of degrees of freedom that may participate in energy redistribution. Figure 6 shows that the ligation of $(c\text{-C}_5\text{H}_5)\text{Mg}^+$ proceeds at the collision rate already with ethane.

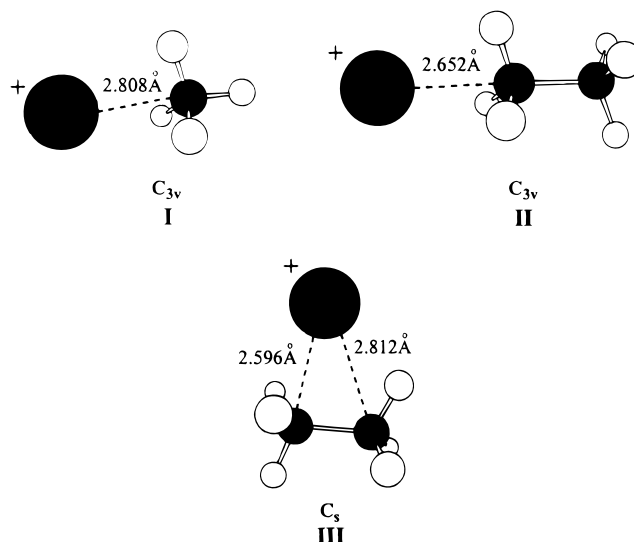
E. Variation in the Rate of Ligation with the Number of $(c\text{-C}_5\text{H}_5)$ Ligands. The results of the measurements reported here show a strong dependence of the rate of ligation with the number of $(c\text{-C}_5\text{H}_5)$ ligands. Although ligation is observed between the bare Mg^+ and hydrocarbons larger than ethane, single ligation of Mg^+ with $c\text{-C}_5\text{H}_5$ enhances reactivity by more than 3 orders of magnitude with methane and ethane. This increase in the rate of ligation is attributed to increased collisional stabilization as a consequence of an increase in the lifetime of the intermediate complex. Clearly, the $(c\text{-C}_5\text{H}_5)$ substituent adds sufficient degrees of freedom to the transient intermediate in the ligation reaction to enhance very substantially the number of degrees of freedom effective in intramolecular energy redistribution, and so, its lifetime. The influence of the $(c\text{-C}_5\text{H}_5)$ ligand on the $(c\text{-C}_5\text{H}_5)\text{Mg}^+ \text{--} \text{RH}$ bond energy is not known, but as discussed later, the multicollision CID experiments suggest an increase in bond energy with $(c\text{-C}_5\text{H}_5)$ ligation, and this also would act to increase the lifetime of the transient intermediate.

No ligation was observed with the "full-sandwich" magnesocene cation nor was there any evidence for ligand switching. The Mg^+ core in the full-sandwich cation appears to be coordinatively saturated, and we take this to account for the observed inertness of the full sandwich to further ligation. The observed nonreactivity of the full-sandwich cation also suggests that strong bonding of any of the ligands investigated with the $c\text{-C}_5\text{H}_5$ ring substituents themselves is not occurring.

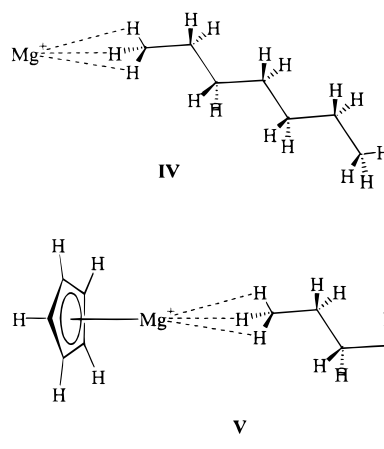
F. Structures and Bonding. Our CID experiments indicate that the ligands that were observed to add to Mg^+ and to $(c\text{-C}_5\text{H}_5)\text{Mg}^+$ can be removed by multicollision-induced dissociation. Production of MgL^+ in the CID of $(c\text{-C}_5\text{H}_5)\text{MgL}^+$ was not observed over the available range in CID energy. Apparently, the $(c\text{-C}_5\text{H}_5)\text{Mg}^+ \text{--} \text{L}$ bond is the weaker bond in each case. Also, it is observed generally that $D(\text{Mg}^+ \text{--} \text{RH}) < D(\text{MgCp}^+ \text{--} \text{RH})$.

The theoretical studies of Bauschlicher et al.^{9,10} indicate that the energy of Mg^+ ligation with methane and ethane is small, $D_e = 6.65$ and 9.94 kcal mol⁻¹, respectively,¹⁰ and that the bonding is electrostatic in nature, with Mg^+ binding preferentially to three hydrogen atoms in an "end-on" fashion with C_{3v} symmetry as indicated in structures **I** and **II**. The bridged structure **III** was found to be energetically less favorable by 1.1 kcal mol⁻¹.

As far as we are aware, there are no previous determinations, either experimental or theoretical, of the structures and bonding of Mg^+ ligated with other homologous hydrocarbons or of $(c\text{-C}_5\text{H}_5)\text{MgL}^+$ ligated with any of the saturated hydrocarbons investigated. But, in view of Bauschlicher's results for methane and ethane, it seems reasonable to propose end-on ligation for



all of the ligated Mg^+ and $(c\text{-C}_5\text{H}_5)\text{Mg}^+$ ions observed in this study as illustrated in structures **IV** and **V** for the ligation of



n-heptane. Also, given that the bonding is primarily electrostatic in nature, we can expect the binding energy to scale roughly with the polarizability or size of the hydrocarbon ligand since, for ion-induced dipole interactions, the potential energy is proportional to polarizability. Indeed, Figure 7 shows a clear linear correlation between the measured onset for the multicollision CID of $(c\text{-C}_5\text{H}_5)\text{Mg}^+ \text{--} \text{L}$ with the polarizability of the hydrocarbon ligand, L. The analogous correlation for the CID of $\text{Mg}^+ \text{--} \text{L}$ is less well defined, partly because of the uncertainty associated with the determination of the onset energy for weakly ligated species. The correlation spans a 5-fold change in the $(c\text{-C}_5\text{H}_5)\text{Mg}^+ \text{--} \text{L}$ onset energy for dissociation and a 2-fold change in the $\text{Mg}^+ \text{--} \text{L}$ onset energy for dissociation. If a linear correlation also is applied to the available theoretical $\text{Mg}^+ \text{--} \text{L}$ bond dissociation energies for L = methane and ethane and extrapolated to *n*-propane, the value for $D_e(\text{Mg}^+ \text{--} n\text{-propane})$ is predicted to be between 14 and 17 kcal mol⁻¹. This compares favorably with the absolute determination made in our study of the standard free-energy change for the ligation reaction in eq 5, $\Delta G^\circ = -8.3$ kcal mol⁻¹. A value for ΔS° (ligation) of -25 cal K⁻¹ estimated from the results of our calculations for ΔS° (ligation) of $\text{Mg}^+ \text{--} n\text{-pentane}$ and statistical thermodynamics leads to an approximate value for ΔH° (ligation) and $D_{298}(\text{Mg}^+ \text{--} n\text{-propane})$ at 300 K of approximately -17 and 16 kcal mol⁻¹.

We have explored further the interaction of Mg^+ with *n*-alkanes in a detailed theoretical study of the interaction of

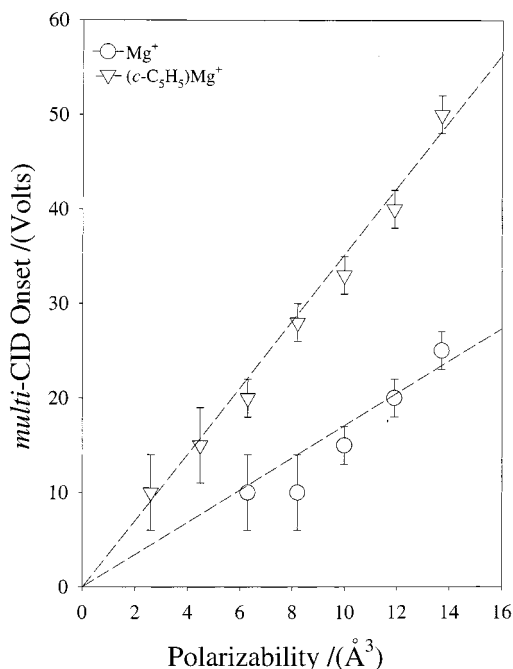


Figure 7. Variation of the measured onset for multicollision-induced dissociation of ligated MgL^+ and $(c\text{-C}_5\text{H}_5)\text{MgL}^+$ in helium buffer-gas at a pressure of 0.35 ± 0.01 Torr with the polarizability of the ligand.

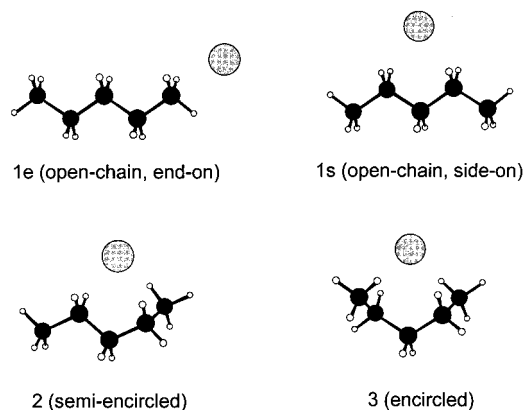


Figure 8. Some isomers of $\text{Mg}^+ - n\text{-pentane}$ calculated at the B3LYP/6-311++G(2d,2p) level of theory.

Mg^+ with $n\text{-pentane}$. Three rotamers were located for pentane (see Figure 8). The enthalpies and free energies of these rotamers at 298 K were found to be within 1.8 and 1.7 kcal mol⁻¹, respectively. Mg^+ has several distinctly different modes of attachment to each of these three rotamers so that the total number of $\text{Mg}^+ - n\text{-pentane}$ isomers is quite large. We calculated the four representative isomers shown in Figure 8. Detailed results are given in Table 2. The most favorable isomer is the linear pentane with Mg^+ attached to its side ($\Delta H_{\text{ligation}} = -17.1$ kcal mol⁻¹, $\Delta G_{\text{ligation}} = -9.9$ kcal mol⁻¹ at 298 K). The likely reason for this is the bonding of Mg^+ to four hydrogen atoms at equal distances (2.317 Å).

To estimate the energy required to move the Mg^+ cation along the chain, we considered rotation of the cation around one of the (central) C–C bonds. The C–C–C–Mg dihedral angle (involving central carbons) was varied from 0° to 180° in steps of 30°, with all other geometry parameters being re-optimized for each value. This procedure provided an estimate for the Mg^+ shift barrier, ca. 3 kcal mol⁻¹. Hence, interconversion of different isomers of $\text{Mg}^+ - n\text{-C}_5\text{H}_{12}$ should be easy, even at room temperature, and the ligated species should be regarded as more “dynamic” than “static”.

TABLE 2: Values for $D_{298}(\text{Mg}^+ - \text{alkane})$ and Results of B3LYP/6-311++G(2d,2p) Calculations for the Enthalpy (ΔH), Entropy (ΔS), and Free Energy (ΔG) for the Ligation of Mg^+ with Ethane and $n\text{-Pentane}$ at 298 K.

alkane ^b	ΔH	ΔS	ΔG	D_{298}
C_2H_6 , end-on	-10.7	-19.9	-4.8	10.1
C_2H_6 , side-on	-10.5	-18.6	-5.0	9.9
C_5H_{12} , 1s	-17.1	-24.1	-9.9	16.5
C_5H_{12} , 2	-15.6	-23.8	-8.5	15.1
C_5H_{12} , 3	-14.2	-25.8	-6.5	13.6
C_5H_{12} , 1e	-12.9	-19.6	-7.1	12.3

^a ΔH , ΔG , and $D_{298}(\text{Mg}^+ - \text{alkane})$ are in kilocalories per mole, and ΔS is in calories per mole per Kelvins. ^b Structures are indicated in I, II, and Figure 8.

The general observation that $D(\text{Mg}^+ - \text{RH}) < D(\text{MgCp}^+ - \text{RH})$ is suggestive. One might expect charge to be more delocalized in MgCp^+ thus weakening any electrostatic interactions with the attached ligands. This is clearly not the case. A more fitting explanation requires consideration of the electronic structures of Mg^+ and $(c\text{-C}_5\text{H}_5)\text{Mg}^+$. The ground-state configuration of Mg^+ , $[\text{Ne}](3s^1)$, involves a singly occupied 3s highest occupied molecular orbital. This orbital should be large and prevent the close approach of Mg^+ and closed-shell species such as the alkanes, thus reducing electrostatic interaction. In $(c\text{-C}_5\text{H}_5)\text{Mg}^+$, the 3s electron may be shared with the $c\text{-C}_5\text{H}_5$ ligand resulting in a smaller, more highly charged center that facilitates stronger electrostatic interaction with alkanes. This is consistent with the formal description of $(c\text{-C}_5\text{H}_5)\text{Mg}^+$ as $(c\text{-C}_5\text{H}_5)^- \text{Mg}^{2+}$. A very recent theoretical study of this cation indicates an interaction that is typical of an ionic bond and NBO analysis indicates a natural charge of 1.8 for Mg .²⁶ Also, it is relevant to note from Figure 7 that the measured onsets of multicollision-induced dissociation for $(c\text{-C}_5\text{H}_5)\text{Mg}^+ - \text{RH}$ are about 2 times higher than that for $\text{Mg}^+ - \text{RH}$, which also is consistent with electrostatic bonding with the alkane. The full-sandwich $(c\text{-C}_5\text{H}_5)_2\text{Mg}^+$, for which no ligation was observed, probably provides an approaching alkane very little access to concentrated charge.

Conclusions

The application of the SIFT technique has allowed an evaluation of the intrinsic kinetics of ligation of Mg^+ , $(c\text{-C}_5\text{H}_5)\text{Mg}^+$, and $(c\text{-C}_5\text{H}_5)_2\text{Mg}^+$ with a family of homologous saturated linear hydrocarbon ligands at room temperature in helium bath gas at 0.35 Torr. The rates of ligation depend on the degree of ligation with $c\text{-C}_5\text{H}_5$ and the size of the hydrocarbon ligand. Thermalized Mg^+ ions react with increasing efficiency as the size of the hydrocarbon increases. No reaction was observed with methane and ethane, and this can be attributed to low ligand-binding energies and relatively small numbers of degrees of freedom in the ligated complexes. The equilibrium achieved for the ligation of Mg^+ with $n\text{-propane}$ provides a standard free-energy change for this ligation of -8.3 kcal mol⁻¹ and an estimated energy change, $\Delta E^\circ = -17$ kcal mol⁻¹ at 300 K. Single ligation of Mg^+ with $c\text{-C}_5\text{H}_5$ substantially enhances the efficiency of ligation. Double ligation with $c\text{-C}_5\text{H}_5$ substantially reduces the efficiency of ligation: no ligation was observed with the “full-sandwich” magnesocene cation.

A linear correlation exists between the measured thresholds for multicollision-induced dissociation and the polarizability of the hydrocarbon ligand. This is consistent with published calculations that indicate a predominantly electrostatic end-on interaction between Mg^+ and methane and ethane. End-on structures can be recommended on the basis of these calculations

for the remaining Mg^+-L species and the $(c\text{-C}_5\text{H}_5)\text{Mg}^+-\text{L}$ species observed in this study. The detailed theoretical study reported here for the interaction of Mg^+ with three rotamers of *n*-pentane indicates that interconversion of different isomers of $\text{Mg}^+-n\text{-C}_5\text{H}_{12}$ should be easy, even at room temperature, and that the ligated species $\text{Mg}^+-n\text{-C}_5\text{H}_{12}$ is “dynamic” rather than “static”. Stronger bonding (by a factor of about 2) is indicated for $(c\text{-C}_5\text{H}_5)\text{Mg}^+-\text{L}$ by the multicollision CID experiments, and this is consistent with a formal description of $(c\text{-C}_5\text{H}_5)\text{Mg}^+$ as $(c\text{-C}_5\text{H}_5)^-\text{Mg}^{2+}$.

Acknowledgment. We thank Doina Caraiman for assisting in some of the experiments and the reviewers for helpful comments. Continued financial support from the Natural Science and Engineering Research Council of Canada is greatly appreciated.

References and Notes

- (1) Ferguson, E. E.; Fehsenfeld, F. C. *J. Geophys. Res.* **1968**, *73*, 6215.
- (2) Isotomin, V. G. *Space Res.* **1963**, *3*, 209.
- (3) Rowe, B. R.; Fahey, D. W.; Ferguson, E. E.; Fehsenfeld, F. C. *J. Chem. Phys.* **1981**, *75*, 3325.
- (4) For example, see: Baggaley, W. J.; Cummack, C. H. *J. Atmos. Terr. Phys.* **1974**, *26*, 1759.
- (5) Kawaguchi, K.; Kagi, E.; Hirano, T.; Takano, S.; Saito, S. *Astrophys. J.* **1993**, *406*, L39.
- (6) For example, see: Lyons, J. R. *Science* **1995**, *267*, 648.
- (7) Operti, L.; Tews, E. C.; MacMahon, T. J.; Freiser, B. S. *J. Am. Chem. Soc.* **1989**, *111*, 9152.
- (8) Linder, C. B.; Dalton, A. L.; Babcock, L. M. *Proceedings of the 43rd ASMS Conference on Mass Spectrometry and Allied Topics*, Atlanta, Georgia, May 21–26, 1995.
- (9) Bauschlicher, C. W., Jr.; Sodupe, M. *Chem. Phys. Lett.* **1993**, *214*, 489.
- (10) Partridge, H.; Bauschlicher, C. W., Jr. *J. Phys. Chem.* **1992**, *96*, 8827.
- (11) Milburn, R. K.; Baranov, V. I.; Hopkinson, A. C.; Bohme, D. K. *J. Phys. Chem.* **1998**, *102*, 9803.
- (12) Milburn, R. K.; Baranov, V. I.; Hopkinson, A. C.; Bohme, D. K. *J. Phys. Chem.* **1999**, *103*, 6373.
- (13) For example, see: Tonkyn, R.; Roman, M.; Weisshaar, J. C. *J. Phys. Chem.* **1988**, *92*, 92.
- (14) Baranov, V. I.; Bohme, D. K. *Int. J. Mass Spectrom. Ion Processes* **1996**, *154*, 71.
- (15) MacKay, G. I.; Vlachos, G. D.; Bohme, D. K.; Schiff, H. I. *Int. J. Mass Spectrom. Ion Phys.* **1980**, *36*, 259.
- (16) Raksit, A. B.; Bohme, D. K. *Int. J. Mass. Spectrom. Ion Processes* **1983**, *55*, 69.
- (17) Frisch, M. J.; Trucks, G. W.; Schlegel, H. B.; Scuseria, G. E.; Robb, M. A.; Cheeseman, J. R.; Zakrzewski, V. G.; Montgomery, J. A., Jr.; Stratmann, R. E.; Burant, J. C.; Dapprich, S.; Millam, J. M.; Daniels, A. D.; Kudin, K. N.; Strain, M. C.; Farkas, O.; Tomasi, J.; Barone, V.; Cossi, M.; Cammi, R.; Mennucci, B.; Pomelli, C.; Adamo, C.; Clifford, S.; Ochterski, J.; Petersson, A.; Ayala, P. Y.; Cui, Q.; Morokuma, K.; Malick, D. K.; Rabuck, A. D.; Raghavachari, K.; Foresman, J. B.; Cioslowski, J.; Ortiz, J. V.; Stefanov, B. B.; Liu, G.; Liashenko, A.; Piskorz, P.; Komaromi, I.; Gomperts, R.; Martin, R. L.; Fox, D. J.; Keith, T.; Al-Laham, M. A.; Peng, C. Y.; Nanayakkara, A.; Gonzalez, C.; Challacombe, M.; Gill, P. M. W.; Johnson, B. G.; Chen, W.; Wong, M. W.; Andres, J. L.; Head-Gordon, M.; Replogle, E. S.; Pople, J. A. *Gaussian 98*, rev. A5; Gaussian, Inc.: Pittsburgh, 1998.
- (18) Stephens, P. J.; Devlin, F. J.; Chabalowski, C. F.; Frisch, M. J. *J. Phys. Chem.* **1994**, *98*, 1623.
- (19) Becke, A. D. *J. Chem. Phys.* **1993**, *98*, 1372; 5648.
- (20) Lee, C.; Yang, W.; Parr, R. G. *Phys. Rev. B* **1988**, *37*, 785.
- (21) Pople, J. A.; Krishnan, R.; Schlegel, H. B.; Binkley, J. S. *Int. J. Quantum Chem.* **1978**, *14*, 545.
- (22) Bartlett, R. J.; Purvis, G. D. *Int. J. Quantum Chem.* **1978**, *14*, 516.
- (23) Su, T.; Chesnavich, W. J. *J. Chem. Phys.* **1982**, *76*, 5183.
- (24) NIST Chemistry WebBook at <http://webbook.nist.gov/>.
- (25) Gardner, P. J.; Preston, S. R.; Siertsema, R.; Steele, D. *J. Comput. Chem.* **1993**, *14*, 1523.
- (26) Berthelot, J.; Luna, A.; Tortajada, J. *J. Phys. Chem.* **1998**, *102*, 6025.